Theory of valence-band and core-level photoemission from plutonium dioxide

Journal of Physics: Conference Series **592** (2015) 012054 doi:10.1088/1742-6596/592/1/012054

Theory of valence-band and core-level photoemission from plutonium dioxide

Jindřich Kolorenč[1], Agnieszka L. Kozub[1,2] and Alexander B. Shick[1]

[1] Institute of Physics, Academy of Sciences of the Czech Republic, Na Slovance 2, 182 21 Prague, Czech Republic

[2] Faculty of Applied Physics and Mathematics, Gdansk University of Technology, Narutowicza 11/12, 80-233 Gdansk, Poland

E-mail: kolorenc@fzu.cz

Abstract. The correlated-band theory implemented as a combination of the local-density approximation with the dynamical mean-field theory is applied to PuO_2. An insulating electronic structure, consistent with the experimental valence-band photoemission spectra, is obtained. The calculations yield a nonmagnetic ground state that is characterized by a noninteger filling of the plutonium 5f shell. The noninteger filling as well as the satellites appearing in the 4f core-level photoemission spectra originate in a sizable hybridization of the 5f shell with the 2p states of oxygen.

1. Introduction

Plutonium dioxide is a correlations-driven insulator [1, 2] with a temperature independent magnetic susceptibility [3]. It crystallizes in the CaF_2 structure (space group $Fm\bar{3}m$), with eight-coordinated plutonium, and four-coordinated oxygen atoms. Due to the prominent role of electron correlations, the theoretical modeling of the electronic structure of PuO_2 presents numerous challenges.

The conventional Kohn–Sham density-functional theory in the local-density (LDA) and generalized gradient approximations fails to explain the insulating character of the oxide [4]. The band-gap problem was addressed a number of times using orbital-dependent functionals such as the self-interaction corrected LDA [5], LDA+U [6], or the hybrid exchange-correlation functionals [4, 7]. All of these calculations lead to an insulator with large magnetic moments at the plutonium atoms in the ground-state solution, in disagreement with experiments. Such overestimated tendency to magnetism appears to be a rather general shortcoming of static mean-field approximations that build on a single determinant of Kohn–Sham orbitals.

The dynamical mean-field theory (DMFT) is able to describe correlated nonmagnetic phases [8]. This method, in combination with the density-functional theory, was successfully applied to PuO_2 recently [9, 10], and it indeed yields an insulating electronic structure without local magnetic moments [10]. In the present paper, we follow up on our previous study [10] where we employed a crystal-field potential deduced from experiments, and assumed a simplified spherically symmetric hybridization of the plutonium 5f shell with the surrounding states. Here we relax these simplifications and determine the quantities entirely from first principles.

2. Methods

We start our investigation with an LDA calculation [11] of the electronic structure of PuO_2 at the experimental lattice constant 5.396 Å [12] taking into account scalar-relativistic effects as well as the spin-orbital coupling. To this end, we employ the *WIEN2k* package [13] with the following parameters: the radii of the muffin-tin spheres are $R_{\mathrm{MT}}(\mathrm{Pu}) = 2.65\,a_{\mathrm{B}}$ for plutonium atoms and $R_{\mathrm{MT}}(\mathrm{O}) = 1.70\,a_{\mathrm{B}}$ for oxygen atoms, the basis-set cutoff is defined with $R_{\mathrm{MT}}(\mathrm{O}) \times K_{\max} = 8.5$, and the Brillouin zone is sampled with 3375 k points (120 k points in the irreducible wedge). The LDA bands of the plutonium 5f and oxygen 2p origin are subsequently mapped onto a tight-binding model with the aid of the *Wannier90* code [14] in conjunction with the *Wien2wannier* interface [15]. This effective model $\hat{H}_{\mathrm{TB}}$ then serves as a base for the LDA+DMFT calculations.

The dynamical mean-field modeling of correlations among the 5f electrons amounts to adding a local[1]selfenergy $\hat{\Sigma}(z)$ to the 5f shell of each Pu atom in the tight-binding model $\hat{H}_{\mathrm{TB}}$. The selfenergy is taken from an auxiliary impurity model that consists of one fully interacting f shell (the impurity) embedded in a self-consistent non-interacting medium $\left(\hat{H}_{\mathrm{TB}} + \hat{\Sigma}\right)$ [8].

The auxiliary model without the f–f interactions can be written as

$$\hat{H}^{(0)}_{\mathrm{imp}} = \sum_{ij} \left[\mathbb{H}_{\mathrm{loc}}\right]_{ij} \hat{f}^{\dagger}_i \hat{f}_j + \sum_{IJ} \left[\mathbb{H}_{\mathrm{bath}}\right]_{IJ} \hat{b}^{\dagger}_I \hat{b}_J + \sum_{iJ} \Big(\left[\mathbb{V}\right]_{iJ} \hat{f}^{\dagger}_i \hat{b}_J + \left[\mathbb{V}^{\dagger}\right]_{Ji} \hat{b}^{\dagger}_J \hat{f}_i \Big) , \tag{1}$$

where the lower-case indices label the f orbitals and run from 1 to 14, and the upper-case indices label the orbitals of the effective medium that is usually referred to as bath. In the present application, we truncate the bath to contain only 14 orbitals, in which case the local hamiltonian $\mathbb{H}_{\mathrm{loc}}$, the bath hamiltonian $\mathbb{H}_{\mathrm{bath}}$ as well as the hybridization $\mathbb{V}$ are all 14×14 matrices. The truncation is necessitated by the method we employ to solve the impurity model, the exact diagonalization, which cannot handle much larger systems. In insulating oxides like PuO_2, such small bath is nevertheless well justified on the physical grounds: the environment of the plutonium 5f shell is dominated by the oxygen ligands and hence a small impurity model analogous to a ligand-field model should accurately represent the dynamics of the 5f shell and its surroundings.

The parameter matrices $\mathbb{H}_{\mathrm{loc}}$, $\mathbb{H}_{\mathrm{bath}}$ and $\mathbb{V}$ are determined by matching the large z asymptotics of the local Green's function of the impurity model $\hat{H}^{(0)}_{\mathrm{imp}}$,

$$\mathbb{G}_{\mathrm{loc}}(z) = \Big[z\mathbb{I} - \mathbb{H}_{\mathrm{loc}} - \mathbb{V}\big(z\mathbb{I} - \mathbb{H}_{\mathrm{bath}}\big)^{-1}\mathbb{V}^{\dagger} \Big]^{-1}, \quad \left[\mathbb{I}\right]_{ij} = \delta_{ij} \, , \tag{2}$$

to the asymptotics of the local Green's function corresponding to the effective medium $\left(\hat{H}_{\mathrm{TB}} + \hat{\Sigma}\right)$. The procedure follows the steps outlined in [16] with a notable difference that the local hamiltonian $\mathbb{H}_{\mathrm{loc}}$ now contains a strong spin-orbital coupling that does not commute with the cubic hybridization function $\mathbb{V}\big(z\mathbb{I} - \mathbb{H}_{\mathrm{bath}}\big)^{-1}\mathbb{V}^{\dagger}$. Therefore, the problem cannot be simplified to diagonal matrices.

The complete interacting impurity model is defined as $\hat{H}_{\mathrm{imp}} = \hat{H}^{(0)}_{\mathrm{imp}} + \hat{U}$ where $\hat{U}$ is the Coulomb repulsion among the f orbitals,

$$\hat{U} = \frac{1}{2} \sum_{m_1 m_2 m_3 m_4 \sigma\sigma'} U_{m_1 m_2 m_3 m_4} \hat{f}^{\dagger}_{m_1\sigma} \hat{f}^{\dagger}_{m_2\sigma'} \hat{f}_{m_4\sigma'} \hat{f}_{m_3\sigma} - U_{\mathrm{H}} \sum_i \hat{f}^{\dagger}_i \hat{f}_i \, . \tag{3}$$

The matrix elements $U_{m_1 m_2 m_3 m_4}$ are parametrized with the Slater integrals $F_0 = 6.5$ eV, $F_2 = 8.1$ eV, $F_4 = 5.4$ eV and $F_6 = 4.0$ eV. The average Coulomb repulsion $U = F_0$ has the same value as in [9] to facilitate comparison of the calculated spectra, the other integrals are

[1] It has non-vanishing matrix elements only between the states of a given f shell.

chosen to obtain the average exchange $J = 0.7$ eV while keeping the Hartree–Fock ratios F_4/F_2 and F_6/F_2 [17]. The second term in eq. (3) is the double-counting correction that removes the Hartree-like contribution already included in the LDA bandstructure $\hat{H}_{\mathrm{TB}}$. We approximate U_{H} by the so-called fully localized limit $U_{\mathrm{H}} = U(n_f - 1/2) - J(n_f - 1)/2$ [18, 19] where n_f is the self-consistently determined number of 5f electrons.

The selfenergy $\hat{\Sigma}(z)$ of the impurity model $\hat{H}_{\mathrm{imp}}$ is computed using an in-house exact-diagonalization code that combines the implicitly restarted Lanczos method for calculation of the bottom of the many-body spectrum [20] with the band Lanczos method for evaluation of the one-particle Green's function [21]. To lessen the computational demands, the Fock space is reduced in a manner analogous to the method developed for Ce compounds by Gunnarsson and Schönhammer [22]. The many-body basis $|f^n \underline{b}^m\rangle$, where n indicates the number of electrons in the f states and m is the number of holes in the bath states, is truncated at $m \leq N_{\mathrm{h}}$. We find that the quantities of interest are essentially converged when the cutoff N_{h} is three or larger.

2.1. Photoemission spectra

The valence-band photoemission intensity can be estimated using the Fermi's golden rule as

$$w_{\mathrm{v}}(E) \sim \mathrm{Im}\,\mathrm{Tr} \sum_k \Big[(E - \mathrm{i}\gamma_{\mathrm{v}})\hat{I} - \hat{H}_{\mathrm{TB}}(k) - \hat{\Sigma}(E - \mathrm{i}\gamma_{\mathrm{v}}) \Big]^{-1}, \tag{4}$$

where the sum runs over the Brillouin zone, $\hat{I}$ is the identity operator, and γ_{v} models the life-time broadening of the valence states together with the experimental resolution. In addition, the impurity model of the dynamical mean-field theory provides a means to calculate the photoemission from core levels [23–25]. The photoelectron intensity can be approximated by [22, 26]

$$w_{\mathrm{c}}(E) \sim \mathrm{Im}\,\langle \mathrm{g.s.}| \left[\big(E - \mathrm{i}\gamma_c - E_{\mathrm{g.s.}} - \epsilon_{\mathrm{c}}\big)\hat{I} + \hat{H}_{\mathrm{imp}} - U_{\mathrm{cv}} \sum_i \hat{f}_i^\dagger \hat{f}_i \right]^{-1} |\mathrm{g.s.}\rangle\,, \tag{5}$$

where $|\mathrm{g.s.}\rangle$ is the ground state of $\hat{H}_{\mathrm{imp}}$, $E_{\mathrm{g.s.}}$ is the corresponding ground-state energy, and γ_{c} simulates the life-time broadening of the core state. The term $-U_{\mathrm{cv}} \sum_i \hat{f}_i^\dagger \hat{f}_i$ represents the Coulomb attraction between the core hole and the 5f electrons, and ϵ_{c} is the energy of the core electron that is removed in the final state. The many-body satellites appear in the core spectra because the initial state of the photoemission process $|\mathrm{g.s.}\rangle$ is not an eigenstate of the final-state hamiltonian $\big(\hat{H}_{\mathrm{imp}} - U_{\mathrm{cv}} \sum_i \hat{f}_i^\dagger \hat{f}_i - \epsilon_{\mathrm{c}}\hat{I}\big)$ due to non-commutativity of the number operator $\hat{f}_i^\dagger \hat{f}_i$ with the hybridization terms $\hat{f}_i^\dagger \hat{b}_J$ and $\hat{b}_J^\dagger \hat{f}_i$.

3. Results

3.1. Valence-band spectrum

The theoretical spectrum of PuO_2 is shown in figure 1 for two values of the life-time broadening γ_{v}. The smaller value is used to visualize the band gap that comes out as 2.5 eV. This gap agrees rather well with 2.8 eV found in recent measurements of optical absorption [2], which justifies our choice of Coulomb $U = 6.5$ eV. The spectrum calculated with the larger broadening is compared with the experimental photoemission measured with incident photons of energy 40.8 eV (He II line) [27]. At this energy, the photoionization cross section for plutonium 5f and oxygen 2p states is approximately the same and hence the photoelectron intensity corresponds to the total spectrum. The spectrum has three main features that are satisfactorily reproduced by the theory. The calculations place these features at energies -1.7 eV, -3.2 eV and -5.0 eV. An inspection of the orbitally resolved spectra indicates that the shoulder at -1.7 eV is dominated by the 5f states

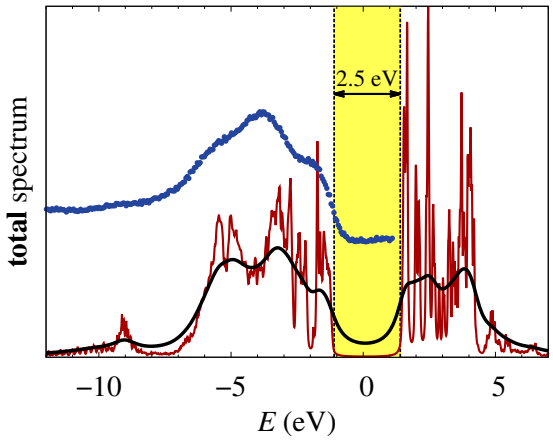

Figure 1. Valence spectrum w_{v} from eq. (4) with broadening $\gamma_{\mathrm{v}} = 0.02$ eV (——) and $\gamma_{\mathrm{v}} = 0.4$ eV (——). The experimental data (•••) taken with incident photon energy 40.8 eV (He II line) [27] are shown for comparison.

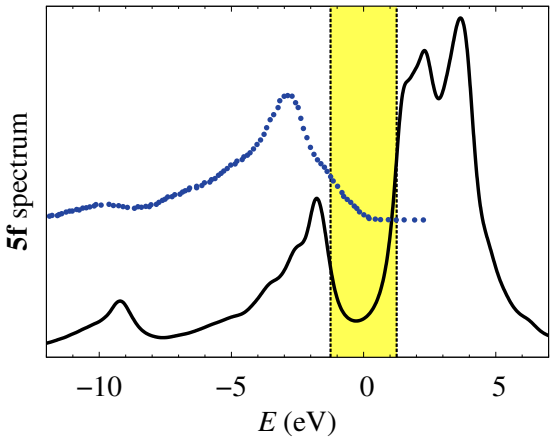

Figure 2. 5f component of the valence-band spectrum calculated with broadening $\gamma_{\mathrm{v}} = 0.4$ eV (——) is compared to the experiment (•••) performed at incident photon energy 1487 eV (aluminum K_α line) [28].

whereas the other two peaks are due to the 2p states. This assignment is further corroborated by photoemission spectra measured at high photon energy (1487 eV, aluminum K_α line) [28] where only the 5f states contribute. The experiment also detects a satellite of the 5f origin that our calculations put at approximately −9.0 eV; the experimental spectrum appears to be shifted by about 1 eV to higher binding energies.

3.2. 4f spectrum

From the hybrid density-functional calculations [4, 7] it was inferred that there is a large covalent mixing of the plutonium 5f states with the 2p states of oxygen. Evidence of such mixing is found also in the core-level spectroscopy [28, 29]. Its theoretical interpretation [30] indicates that the filling of the plutonium 5f shell noticeably departs from the nominal integer occupation $n_f = 4$ associated with the Pu^{4+} ion.

Our calculations yield $n_f \approx 4.4$ which is in line with the earlier studies although slightly smaller than $n_f = 4.65$ deduced in [30]. The comparison of the 4f photoemission spectra obtained

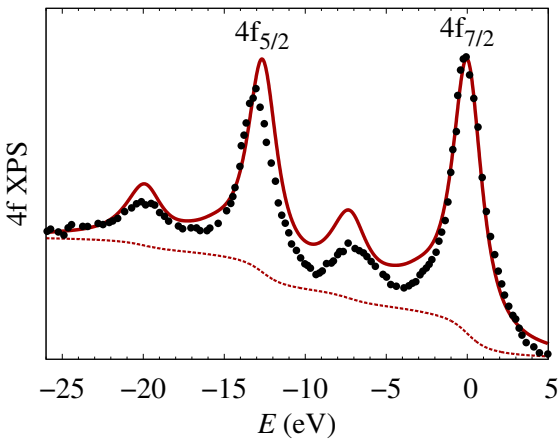

Figure 3. Photoemission from the plutonium 4f levels calculated as a superposition of two spectra from eq. (5) weighted with the statistical ratio 4/3 (——). The $4f_{5/2} - 4f_{7/2}$ splitting is taken from the LDA calculation (12.64 eV), the core-valence potential U_{cv} is set to 6 eV, and the broadening γ_{c} is adjusted to match the width of the $4f_{7/2}$ line in the experimental spectrum (•••) [29]. The calculated and experimental spectra are aligned at the $4f_{7/2}$ line, and a background due to secondarily scattered electrons (----) is added to the theoretical curve as described in [30].

Table 1. Parameters of the local hamiltonian $\mathbb{H}_{\rm loc}$, and the first three excitation energies (the number in brackets indicates the degeneracy of the excited state). Our calculations are compared with results of two other methods. The states $\Gamma_5(3)$ and $\Gamma_3(2)$ are interchanged in our calculations compared to LDA+U [32]. All energies are listed in meV.

	ξ	V_4	V_6	$\Gamma_4(3)$	$\Gamma_5(3)$	$\Gamma_3(2)$
inelastic neutrons [31]	300	−151	31	124		
LDA+U [32]	304	−99	17	97	204	195
present study	322	−39	12	125	226	319

experimentally [29] and calculated from eq. (5), figure 3, shows that our modeling of the local electronic structure at the plutonium atom is sufficiently accurate. In particular, the satellites that originate from the hybridization with the oxygen ligand states are well reproduced without any fitting of the hybridization strength – it comes directly from the LDA+DMFT calculations.

3.3. Crystal-field states

Finally, we discuss the role of the cubic environment around the plutonium atoms. Its most important implication is the absence of magnetism [3] – the crystal-field potential and the hybridization split the 5f states such that the ground state is non-degenerate. The first excited state is a triplet and it was found at 124 meV above the ground state in inelastic neutron scattering [31]. The first excitation in our impurity model $\hat{H}_{\rm imp}$ turns out to be at 125 meV which is an excellent agreement but more compounds will have to be tested to check whether such accuracy is systematic or somewhat fortuitous.

To analyze the splitting in more detail, we decompose the local hamiltonian $\mathbb{H}_{\rm loc}$ into a sum of the spin-orbital term $\xi(\mathbf{l}\cdot\mathbf{s})$ and the cubic crystal-field potential

$$V_{\rm CF} = \frac{16\sqrt{\pi}}{3} V_4 \left[Y_{40}(\theta,\varphi) + \sqrt{\frac{10}{7}}\,\mathrm{Re}\,Y_{44}(\theta,\varphi) \right] + 32\sqrt{\frac{\pi}{13}} V_6 \left[Y_{60}(\theta,\varphi) - \sqrt{14}\,\mathrm{Re}\,Y_{64}(\theta,\varphi) \right], \quad (6)$$

where $Y_{lm}(\theta,\varphi)$ are spherical harmonics. The parameters ξ, V_4 and V_6 are compared in table 1 with values estimated by other methods: the inelastic neutron scattering experiments [31] and the LDA+U method combined with the crystal-field model [32]. Apparently, our V_4 and V_6 are not directly comparable to the values from the literature. The reason is that we employ an impurity model that explicitly includes the hybridization with ligands whereas the other studies work with a simpler crystal-field model where the hybridization term is absent and its effect is folded into the crystal-field potential. By switching off the hybridization while keeping our small values of V_4 and V_6 we find that the hybridization is responsible for approximately half of the splitting due to the cubic environment.

4. Conclusions

We have demonstrated that a variant of the LDA+DMFT method where the selfenergy is obtained by exact diagonalization of a finite impurity model similar to the multiplet ligand-field model provides an accurate and comprehensive description of the electronic structure of the plutonium dioxide. A nonmagnetic insulator is obtained, and the main features of the valence-band as well as core-level photoemission spectra are well reproduced. The method allows us to quantitatively analyze the effects of hybridization between the plutonium 5f and oxygen 2p states from first principles.

Acknowledgments

We acknowledge financial support from the Czech Republic Grant GACR P204/10/0330. A. L. K. acknowledges financial support from the International Visegrad Fund within the research project No. 51301118. Access to computing and storage facilities owned by parties and projects contributing to the National Grid Infrastructure MetaCentrum, provided under the programme "Projects of Large Infrastructure for Research, Development, and Innovations" (LM2010005), is greatly appreciated.

References

[1] McNeilly C E 1964 *J. Nucl. Mater.* **11** 53–58
[2] McCleskey M T, Bauer E, Jia Q, Burrell A K, Scott B L, Conradson S D, Mueller A, Roy L, Wen X, Scuseria G E and Martin R L 2013 *J. Appl. Phys.* **113** 013515
[3] Raphael G and Lallement R 1968 *Solid State Commun.* **6** 383–385
[4] Wen X D, Martin R L, Henderson T M and Scuseria G E 2013 *Chem. Rev.* **113** 1063–1096
[5] Petit L, Svane A, Szotek Z, Temmerman W M and Stocks G M 2010 *Phys. Rev. B* **81** 045108
[6] Suzuki M T, Magnani N and Oppeneer P M 2013 *Phys. Rev. B* **88** 195146
[7] Wen X D, Martin R L, Roy L E, Scuseria G E, Rudin S P, Batista E R, McCleskey T M, Scott B L, Bauer E, Joyce J J and Durakiewicz T 2012 *J. Chem. Phys.* **137** 154707
[8] Georges A, Kotliar G, Krauth W and Rozenberg M J 1996 *Rev. Mod. Phys.* **68** 13–125
[9] Yin Q, Kutepov A, Haule K, Kotliar G, Savrasov S Y and Pickett W E 2011 *Phys. Rev. B* **84** 195111
[10] Shick A B, Kolorenč J, Havela L, Gouder T and Caciuffo R 2014 *Phys. Rev. B* **89** 041109
[11] Perdew J P and Wang Y 1992 *Phys. Rev. B* **45** 13244–13249
[12] Villars P 1997 *Pearson's Handbook Desk Edition: Crystallographic Data for Intermetallic Phases* (ASM International, Materials Park, Ohio)
[13] Blaha P, Schwarz K, Madsen G K H, Kvasnicka D and Luitz J 2001 *WIEN2k, An Augmented Plane Wave + Local Orbitals Program for Calculating Crystal Properties* (Techn. Universität Wien, Austria)
[14] Mostofi A A, Yates J R, Lee Y S, Souza I, Vanderbilt D and Marzari N 2008 *Comput. Phys. Commun.* **178** 685–699
[15] Kuneš J, Arita R, Wissgott P, Toschi A, Ikeda H and Held K 2010 *Comput. Phys. Commun.* **181** 1888–1895
[16] Kolorenč J, Poteryaev A I and Lichtenstein A I 2012 *Phys. Rev. B* **85** 235136
[17] Moore K T and van der Laan G 2009 *Rev. Mod. Phys.* **81** 235–298
[18] Czyżyk M T and Sawatzky G A 1994 *Phys. Rev. B* **49** 14211–14228
[19] Solovyev I V, Dederichs P H and Anisimov V I 1994 *Phys. Rev. B* **50** 16861–16871
[20] Lehoucq R B, Sorensen D C and Yang C 1998 *ARPACK Users' Guide, Solution of Large-Scale Eigenvalue Problems with Implicitly Restarted Arnoldi Methods* (SIAM, Philadelphia, PA)
[21] Meyer H D and Pal S 1989 *J. Chem. Phys.* **91** 6195–6204
[22] Gunnarsson O and Schönhammer K 1983 *Phys. Rev. B* **28** 4315–4341
[23] Kim H D, Noh H J, Kim K H and Oh S J 2004 *Phys. Rev. Lett.* **93** 126404
[24] Cornaglia P S and Georges A 2007 *Phys. Rev. B* **75** 115112
[25] Hariki A, Ichinozuka Y and Uozumi T 2013 *J. Phys. Soc. Jpn.* **82** 023709
[26] de Groot F and Kotani A 2008 *Core Level Spectroscopy of Solids* (CRC Press, Boca Raton, FL)
[27] Gouder T, Shick A and Huber F 2013 *Topics in Catalysis* **56** 1112–1120
[28] Teterin Y A, Maslakov K I, Teterin A Y, Ivanov K E, Ryzhkov M V, Petrov V G, Enina D A and Kalmykov S N 2013 *Phys. Rev. B* **87** 245108
[29] Veal B W, Lam D J, Diamond H and Hoekstra H R 1977 *Phys. Rev. B* **15** 2929–2942
[30] Kotani A and Yamazaki T 1992 *Prog. Theor. Phys. Supplement* **108** 117–131
[31] Kern S, Robinson R A, Nakotte H, Lander G H, Cort B, Watson P and Vigil F A 1999 *Phys. Rev. B* **59** 104–106
[32] Zhou F and Ozoliņš V 2012 *Phys. Rev. B* **85** 075124